Supplementary Information for:

The AWAKEN wind farm benchmark. Part 2: modeling results

Nicola Bodini et al.

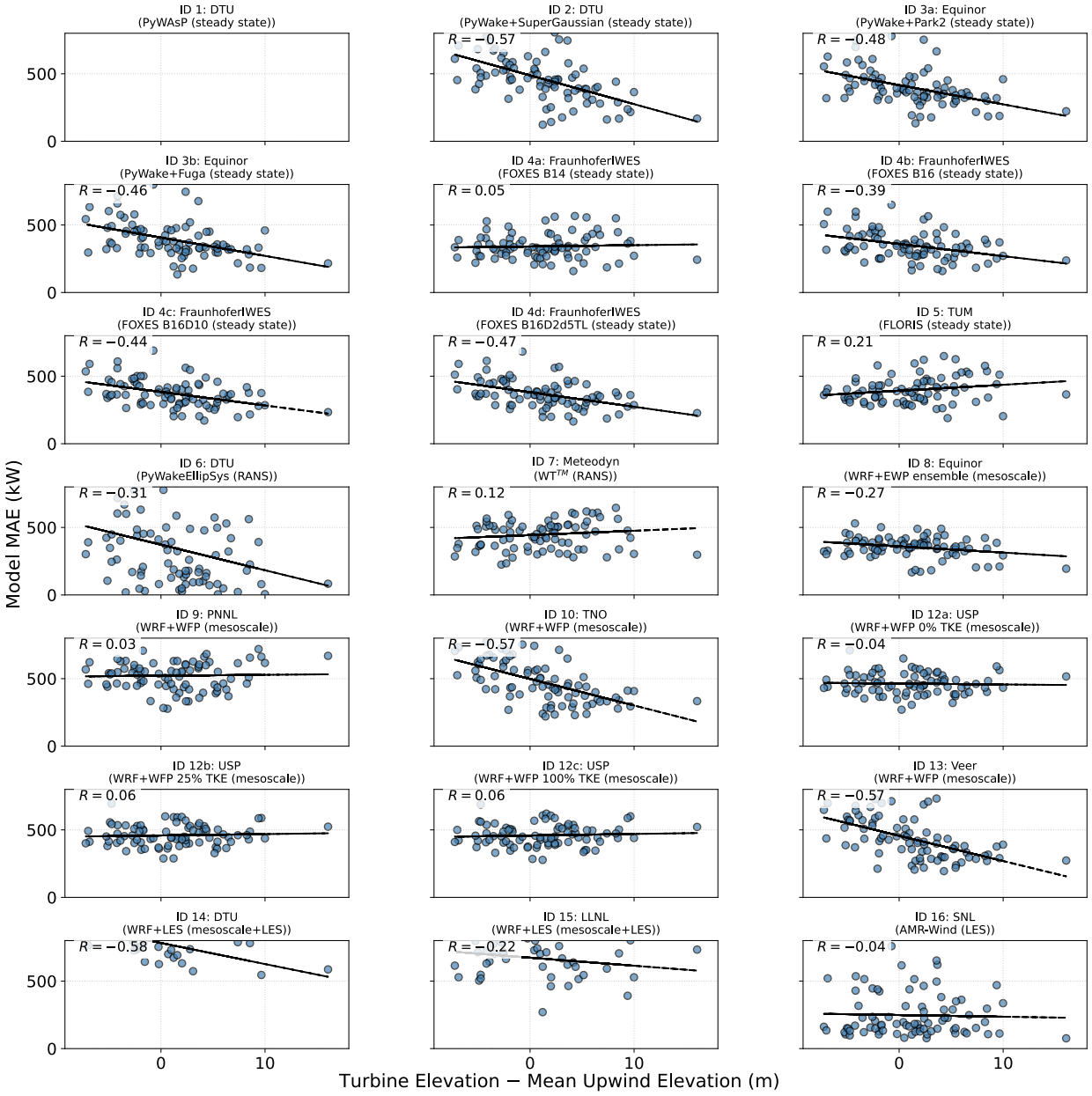

Figure S1. Scatterplots of turbine-level Mean Absolute Error (MAE) versus relative terrain elevation for each Phase 1 model submission (stable conditions only).

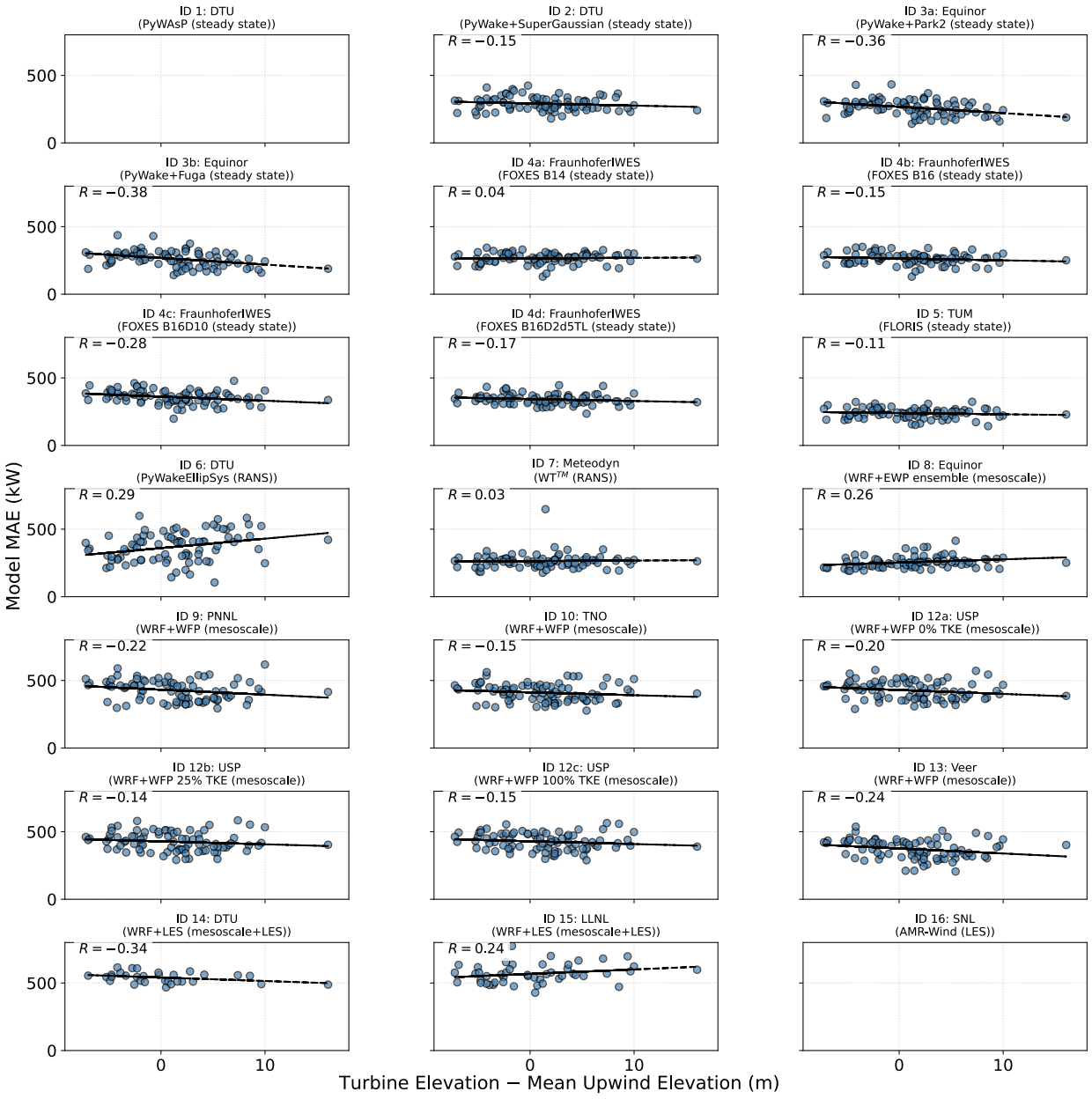

Figure S2. Scatterplots of turbine-level Mean Absolute Error (MAE) versus relative terrain elevation for each Phase 1 model submission (unstable conditions only).

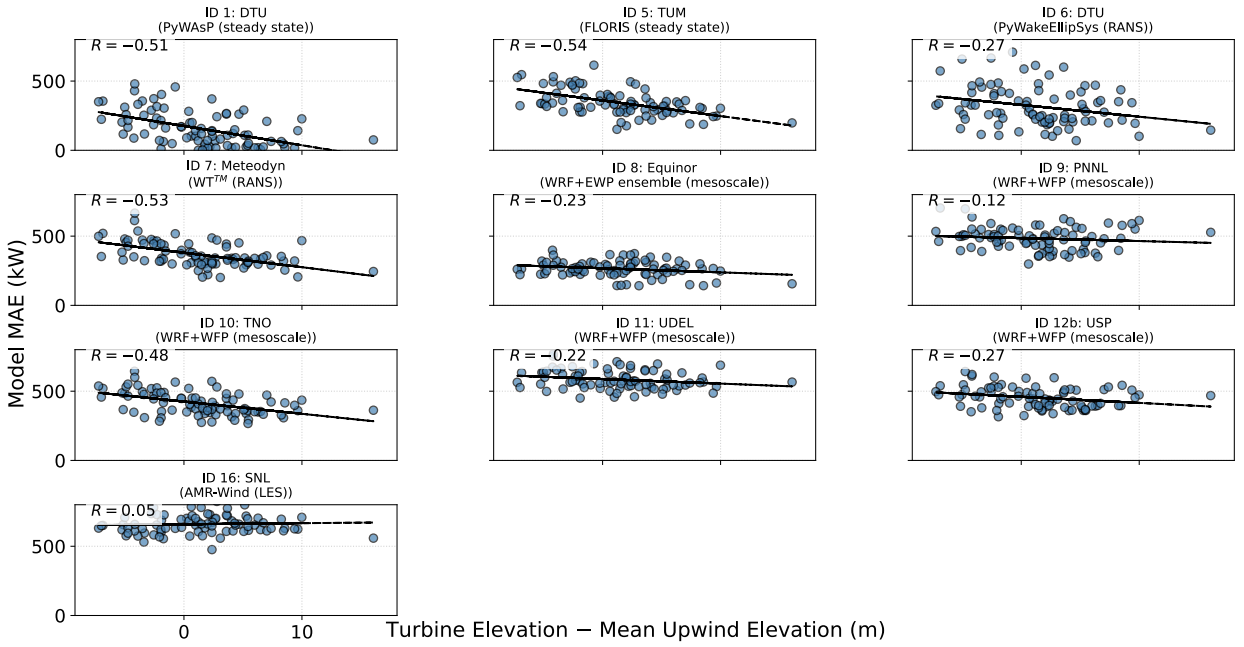

Figure S3. Scatterplots of turbine-level Mean Absolute Error (MAE) versus relative terrain elevation for each Phase 2 model submission.

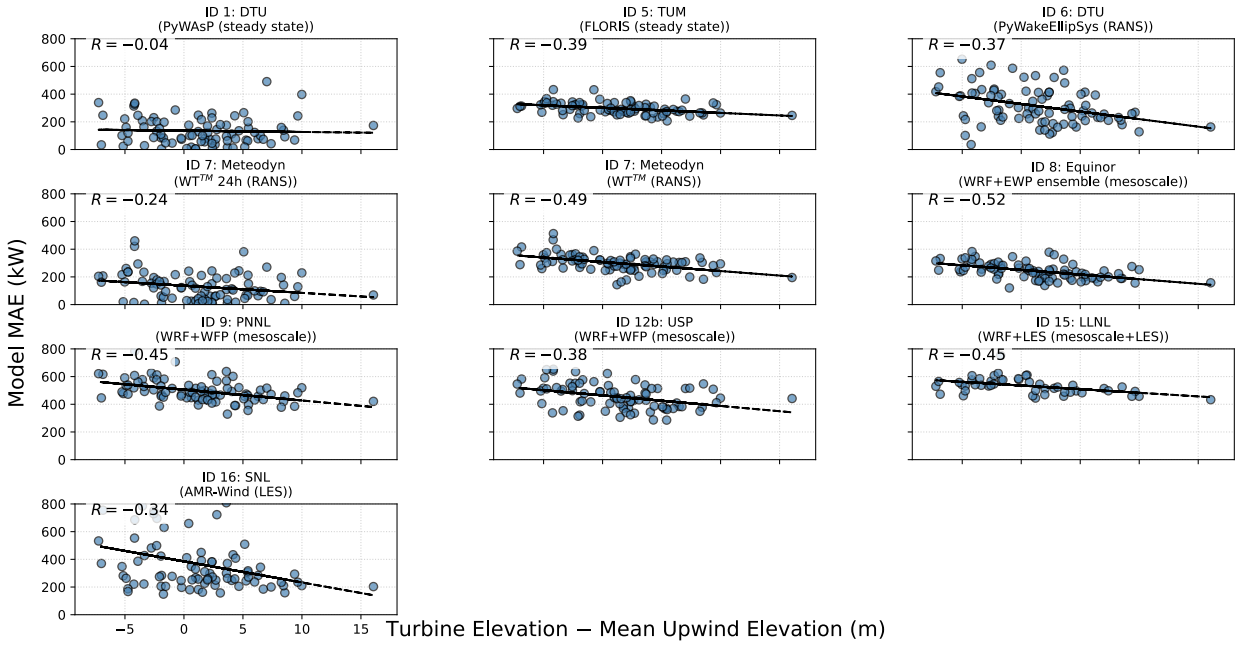

Figure S4. Scatterplots of turbine-level Mean Absolute Error (MAE) versus relative terrain elevation for each Phase 3 model submission.

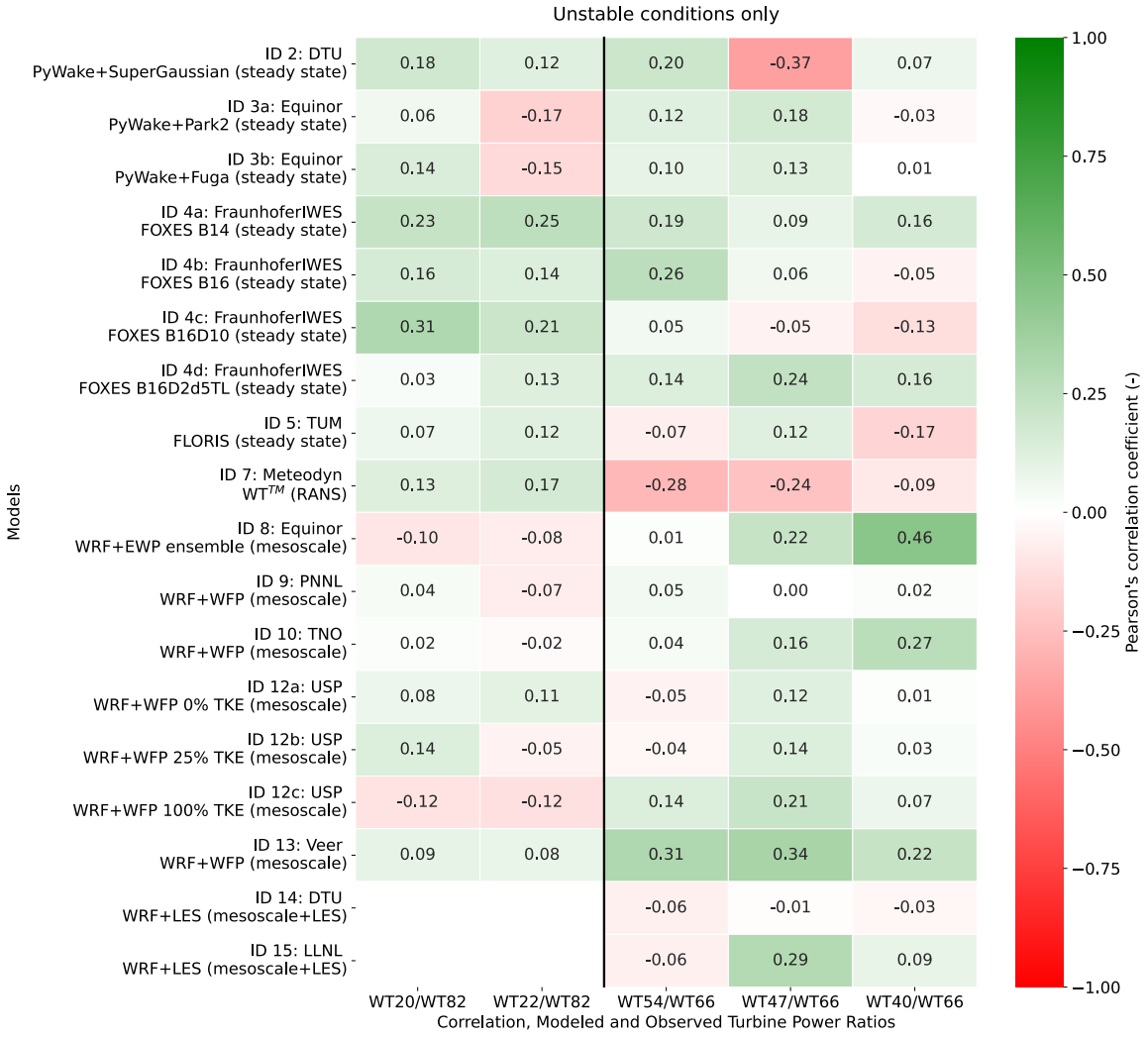

Figure S5. Pearson correlation coefficients between observed and modeled power ratios between turbine pairs during Phase 1, calculated using only data from unstable atmospheric conditions, for turbines in the western (left) and eastern (right) portions of King Plains.

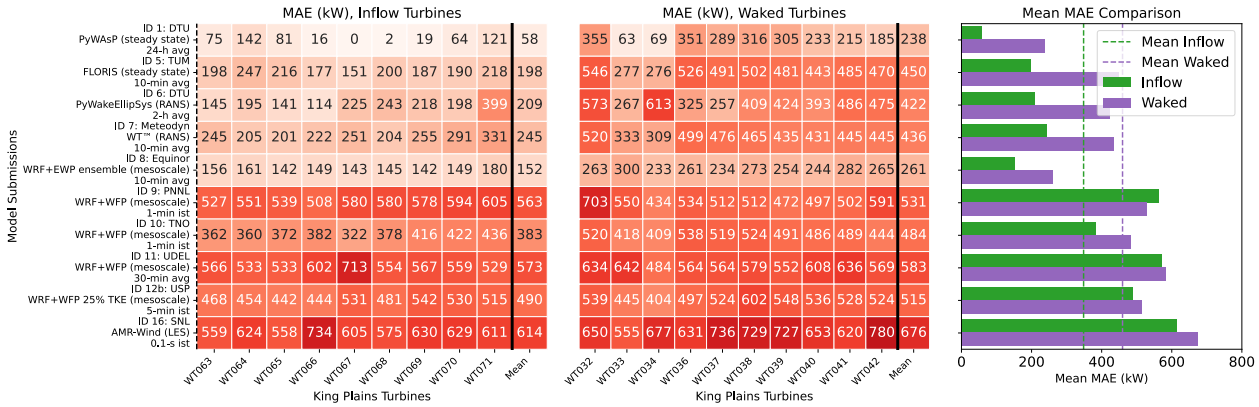

Figure S6. MAE in modeled power for selected turbines in the southern (inflow) row of King Plains (left) and the northern (waked) row (middle). The bar chart on the right compares the mean MAE across all submissions for inflow versus waked turbines. Results for phase 2.

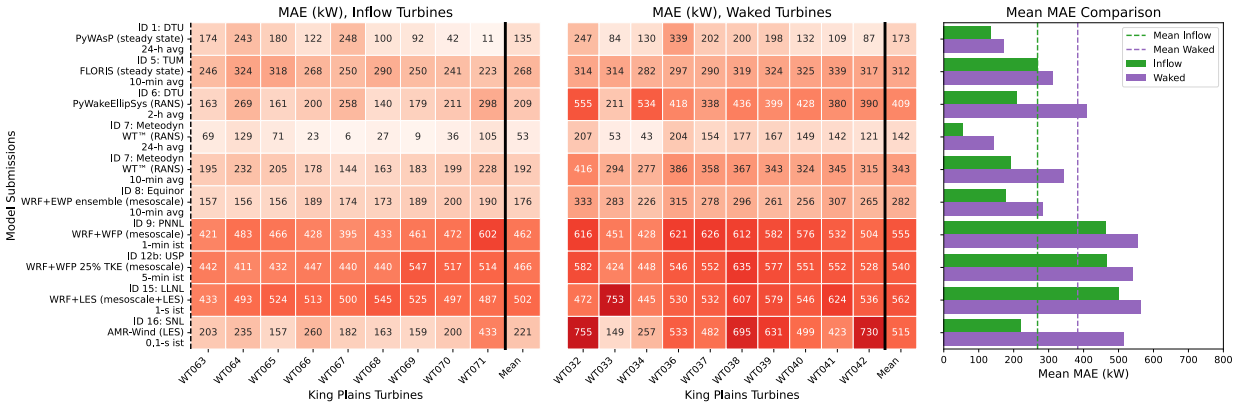

Figure S7. MAE in modeled power for selected turbines in the southern (inflow) row of King Plains (left) and the northern (waked) row (middle). The bar chart on the right compares the mean MAE across all submissions for inflow versus waked turbines. Results for phase 3.

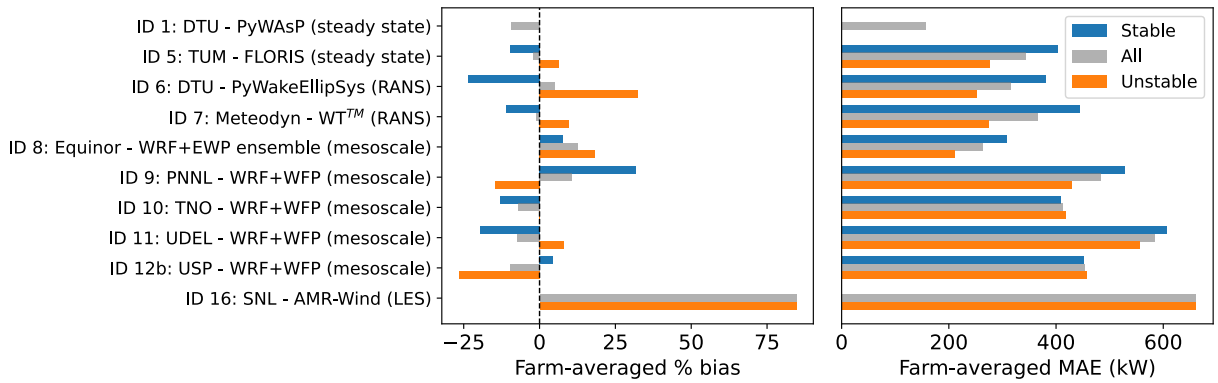

Figure S8. Histograms showing the farm-averaged percent bias (left) and mean absolute error (right) in modeled vs observed power produced by the King Plains wind plant on 24 August 2023 for each model submission to Phase 2 of the benchmark.

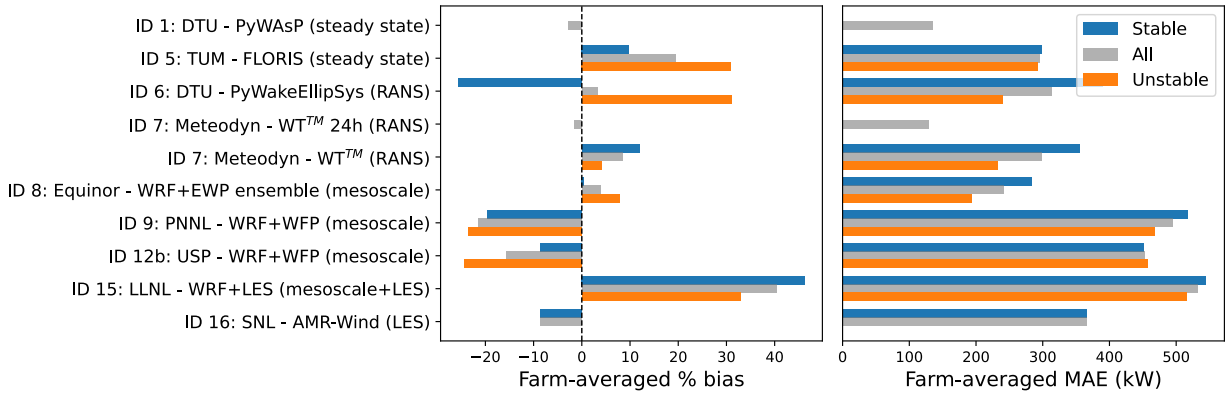

Figure S9. Histograms showing the farm-averaged percent bias (left) and mean absolute error (right) in modeled vs observed power produced by the King Plains wind plant on 24 August 2023 for each model submission to Phase 3 of the benchmark.

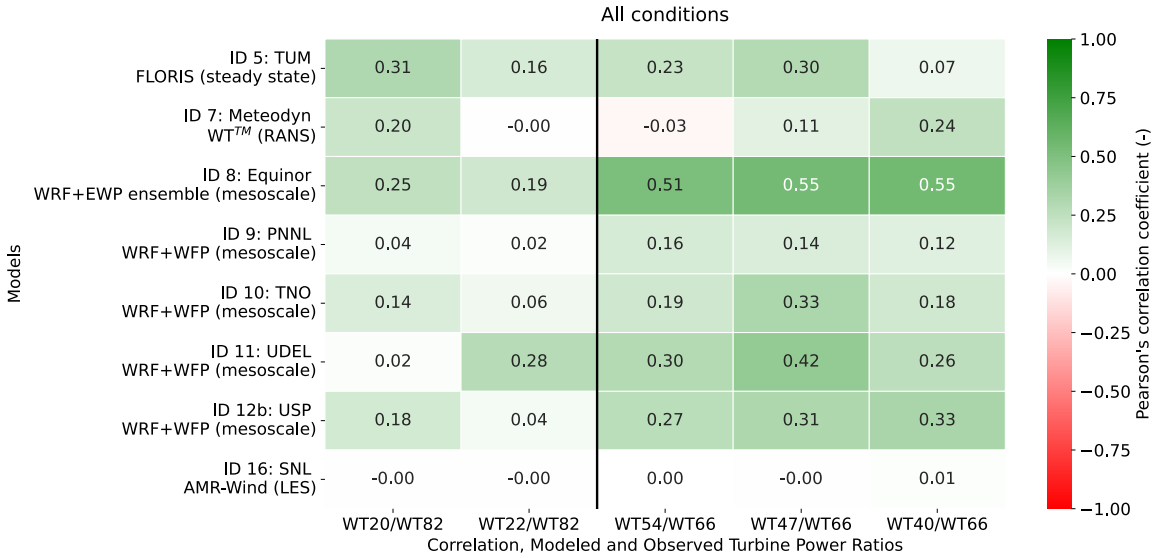

Figure S10. Pearson correlation coefficients between observed and modeled power ratios for selected turbine pairs during Phase 2. The ratios are calculated as the power of the waked turbine divided by the power of a corresponding upstream reference turbine in the southernmost row, for turbines in the western (left) and eastern (right) portions of King Plains.

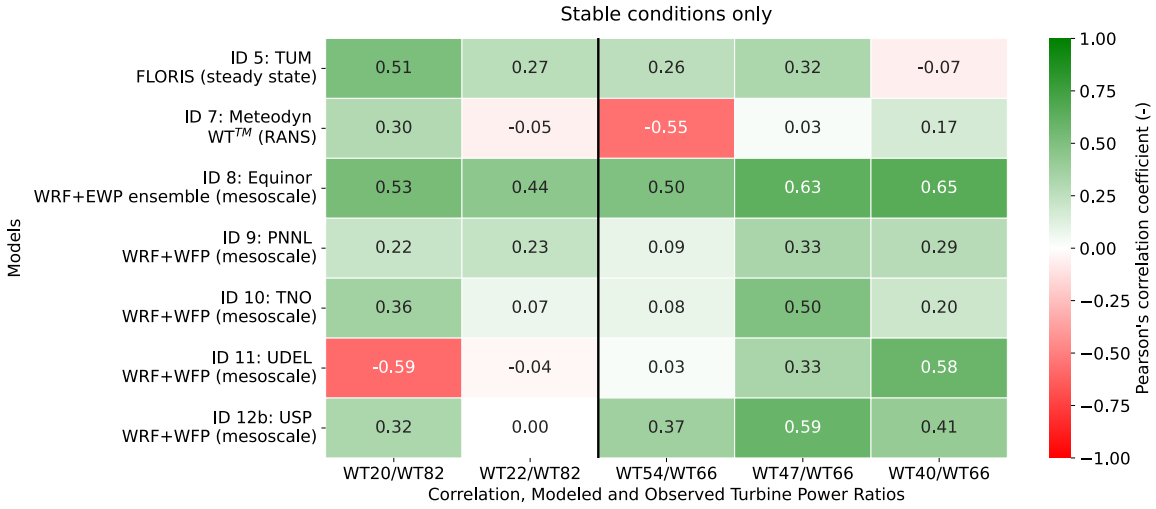

Figure S11. Pearson correlation coefficients between observed and modeled power ratios between turbine pairs during Phase 2, calculated using only data from stable atmospheric conditions, for turbines in the western (left) and eastern (right) portions of King Plains.

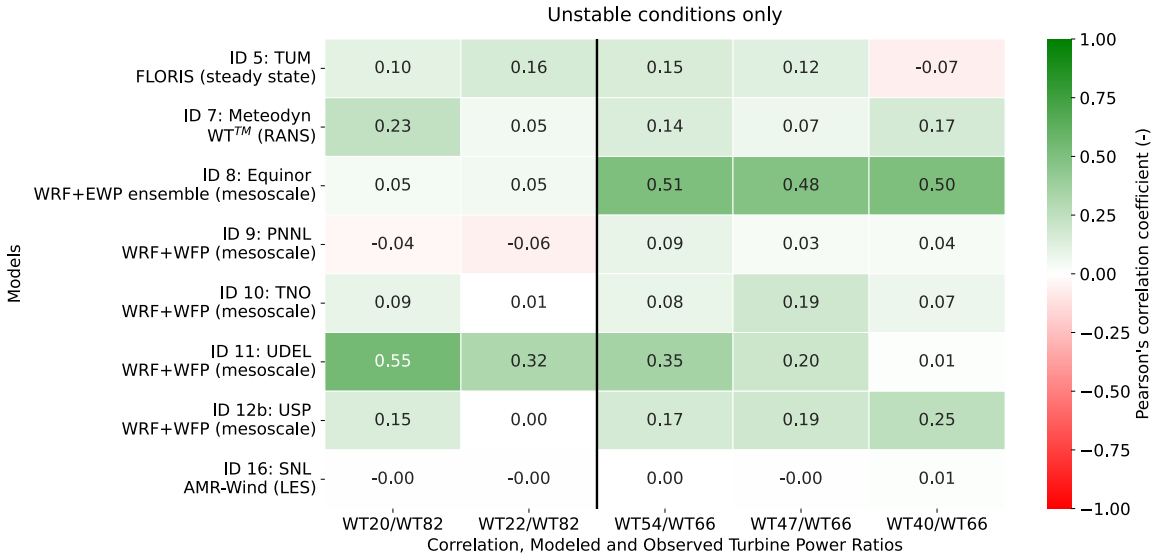

Figure S12. Pearson correlation coefficients between observed and modeled power ratios between turbine pairs during Phase 2, calculated using only data from unstable atmospheric conditions, for turbines in the western (left) and eastern (right) portions of King Plains.

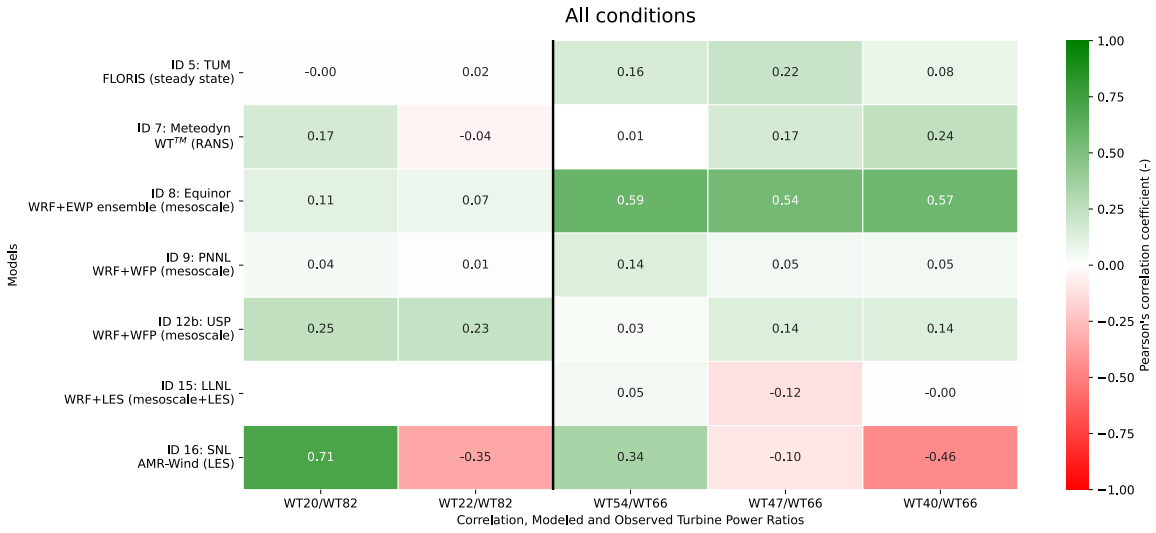

Figure S13. Pearson correlation coefficients between observed and modeled power ratios for selected turbine pairs during Phase 3. The ratios are calculated as the power of the waked turbine divided by the power of a corresponding upstream reference turbine in the southernmost row, for turbines in the western (left) and eastern (right) portions of King Plains.

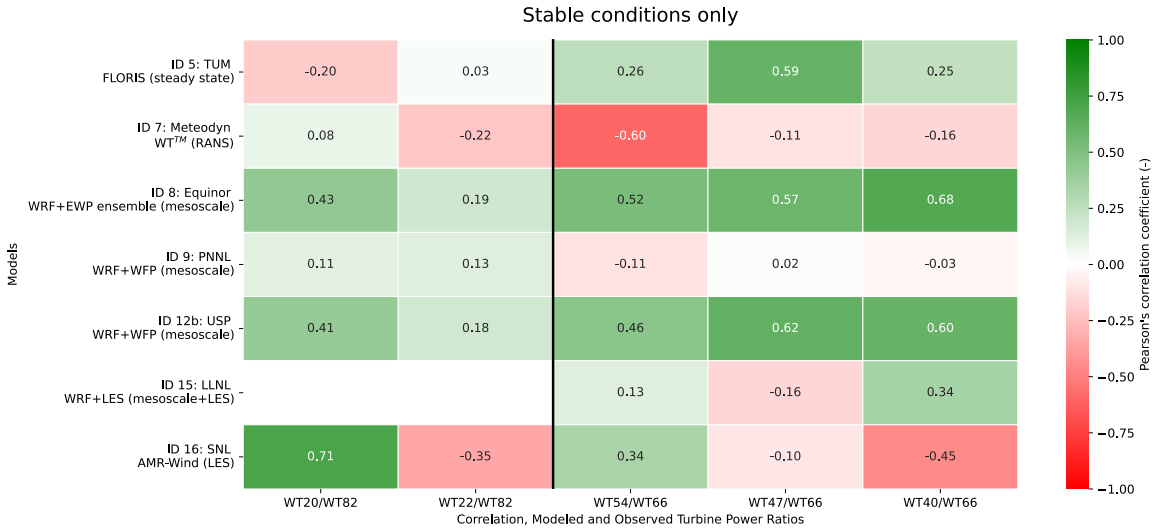

Figure S14. Pearson correlation coefficients between observed and modeled power ratios between turbine pairs during Phase 3, calculated using only data from stable atmospheric conditions, for turbines in the western (left) and eastern (right) portions of King Plains.

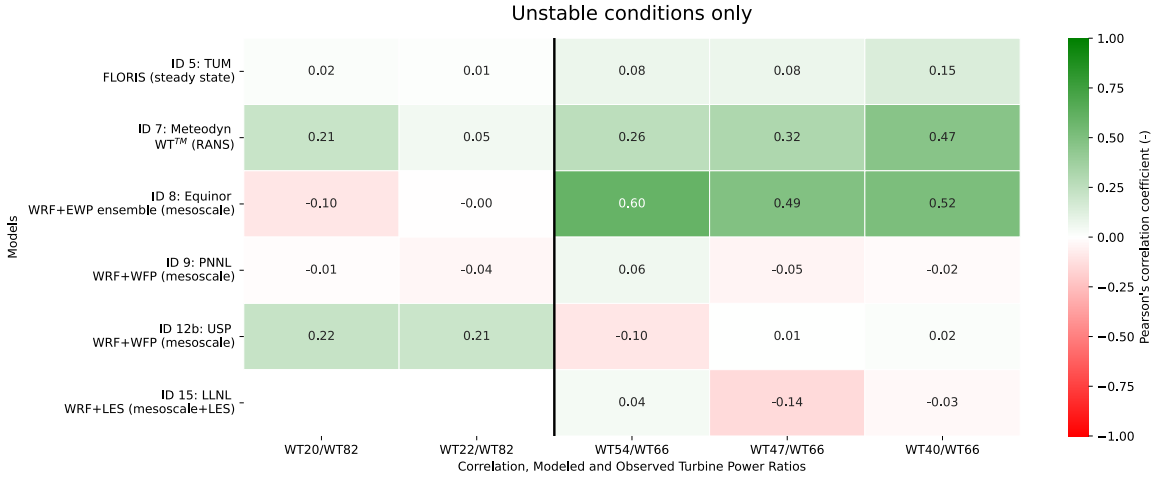

Figure S15. Pearson correlation coefficients between observed and modeled power ratios between turbine pairs during Phase 3, calculated using only data from unstable atmospheric conditions, for turbines in the western (left) and eastern (right) portions of King Plains.